



## Article

# Anti-Inflammatory Nanocarriers Based on SWCNTs and Bioactive Molecules of Oregano: An In Silico Study

Erik Díaz-Cervantes <sup>1,\*</sup>, Alejandra Monjaraz-Rodríguez <sup>1</sup> and Faustino Aguilera-Granja <sup>2</sup>

<sup>1</sup> Departamento de Alimentos, Centro Interdisciplinario del Noreste de la Universidad de Guanajuato, Tierra Blanca, Guanajuato 37975, Mexico

<sup>2</sup> Instituto de Física, Universidad Autónoma de San Luis Potosí, San Luis Potosí 78000, Mexico

\* Correspondence: e.diaz@ugto.mx

**Abstract:** We studied two main bioactive molecules of oregano, carvacrol and thymol, in the present work. These bioactive conformers are linked to single wall carbon nanotubes (SWCNT) and so-called functionalized SWCNT (f-SWCNT) to find their application as anti-inflammatory drugs. We use the multiscale methods and the density functional theory (DFT) of formalism to achieve this aim. We have proposed two nanocarriers based on a finite size model of a metallic single wall carbon nanotube linked to carvacrol and thymol (with a size around 2.74 nm): the main bioactives present in oregano. The results show that the proposed molecules, Carva-SWCNT-Gluc and Thymol-SWCNT-Gluc, can be synthesized with the exposed condensation reaction; with an exergonic and spontaneous behavior, Gibbs free energies of the reaction are  $-1.75$  eV and  $-1.81$  eV, respectively. The studied molecules are subjected to an electronic characterization, considering the global descriptors based on the conceptual DFT formalism. Moreover, the results show that the studied molecules can present a possible biocompatibility due to the higher polarization of the molecule and the increase in apparent solubility. Finally, the interaction between the studied nanodevices (Carva-SWCNT-Gluc and Thymol-SWCNT-Gluc) with cancer and anti-inflammatory targets shows that the hydrogen bond and electrostatic interactions play a crucial role in the ligand–target interaction. The proposed f-SWCNT presents higher potentiality as a carrier vector nanodevice since it can deliver the oregano bioactives on the studied targets, promoting the putative apoptosis of neoplastic cells and simultaneously regulating the inflammatory process.

**Keywords:** nanocarrier; SWCNT; carvacrol; thymol; DFT; multiscale method; cancer; anti-inflammatory



**Citation:** Díaz-Cervantes, E.; Monjaraz-Rodríguez, A.; Aguilera-Granja, F. Anti-Inflammatory Nanocarriers Based on SWCNTs and Bioactive Molecules of Oregano: An In Silico Study. *Nanomanufacturing* **2022**, *2*, 176–185. <https://doi.org/10.3390/nanomanufacturing2040012>

Academic Editor: Xiaojuan Fan

Received: 1 July 2022

Accepted: 27 September 2022

Published: 2 October 2022

**Publisher's Note:** MDPI stays neutral with regard to jurisdictional claims in published maps and institutional affiliations.



**Copyright:** © 2022 by the authors. Licensee MDPI, Basel, Switzerland. This article is an open access article distributed under the terms and conditions of the Creative Commons Attribution (CC BY) license (<https://creativecommons.org/licenses/by/4.0/>).

## 1. Introduction

The use of medicinal plants has been rooted in the whole world; many people would draw on the benefits of natural extracts for numerous ailments, specifically as nutraceuticals. In the past, such activity was considered just as home remedies. Nowadays, several groups have explored the study of essential oils and their healing properties because products derived from plants are expected to induce fewer side effects than synthetic drugs [1]. One of the most studied plants is the oregano species of the family *Lamiaceae*, including the genera *Origanum* and *Thymus* [2]. The most common species in Mexico is the genera *Lippia berlandieri* (or *Lippia graveolens*), which grows in semiarid areas. Other *Lippia* species, such as *Lippia palmeri* or *Lippia alba*, can grow in tropical and temperate climates [3].

The essential oils of oregano species were reported with some beneficial activities because their components have been identified and have a purpose in human health [4]. This essential oil has a higher concentration of monoterpenes. Due to their lipophilic character, compounds can diffuse through the cellular membrane, disrupt the permeability, modify ion influx, and cause structural damage to membrane-bound proteins [5].

That is why the main applications of essential oils are as potential antimicrobial agents [6,7], anti-oxidant [8], anti-inflammatory [9], or even anticancer activity [1,10,11].

Currently, the mechanism of all the compounds in the essential oil are unclear because synergistic or antagonistic behavior can exist in the mixture [12,13]. The above reason is why it is essential to take one by one and obtain accurate information about their mechanisms.

In particular, the present study has focused on two components of this essential oil [14], carvacrol [15] and thymol [16], where natural-bioactive monoterpenes are presented [8]. Both compounds are recognized as safe food additives and have been extensively studied [17]. They are isomers that differ only by the hydroxyl group, which is critical to biological activity [18] because the difference can be significant in how they interact with the environment. For example, the principal mode of action attributed to thymol and carvacrol is linked to the permeability of the cell membrane [5,19,20]. However, it was reported that a mechanism of electron delocalization favored by the –OH group in carvacrol, which enables it to promote membrane depolarization where it dissolves into the phospholipid bilayer and aligns between the fatty acid chains, causes changes in the membrane permeability and therefore the death of microorganisms. Meanwhile, thymol interacts with proteins in the cell membranes, affecting membrane permeability [5,19,21].

In addition to all the previous mechanisms, reports about anticancer and anti-inflammatory effects have been taken for this study where carvacrol [2,22–25], which was reported to have an antiproliferative effect on liver, lung, colon, and breast cancer cell lines, and thymol impact tumor cells mainly through inducing programmed cell death, decreasing cell division, and blocking angiogenesis and metastasis [16,26]. Both molecules have the properties of an anti-inflammatory drug whose properties help anticancer processes.

The drawbacks of natural compounds such as carvacrol and thymol are that they can be unstable and poorly soluble in water [27]. Those characteristics reduce their effectiveness in medical treatments. Many attempts have been made to find new ways to deliver these compounds near the target. For example, by employing liposomes as micelles [28,29], some groups present a possible way to deliver the monoterpenes to the target cells. These groups highlight that liposomes entrap the active compounds in their double lipidic layer, which involves the hydrophilic compounds in an aqueous compartment, and the lipophilic in the double lipidic layer. On the other hand, another methodology present in this study offers devices seeking to yield a more biocompatible vector functionalized single wall carbon nanotubes (f-SWCNTs) [30,31] with molecules that offer higher solubility in water, and at the same time, SWCNT have attached molecules such as carvacrol and thymol. The geometrical optimization and the electronic properties of these nanodevices were computed through the formalism of the density functional theory (DFT) [32,33], at level PBE/6-311G(d,p) [34,35]. With the selected molecules at the specified level of theory, we computed the model of two drug transport nanodevices with possible anticancer and anti-inflammatory effects.

## 2. Computational Methods

### 2.1. Functionalization, Binding Energies, and Chemical Descriptors

A single wall carbon nanotube was modeled considering a finite size whose edges were capped with hydrogen atoms in the tips to avoid dangling bonds in the molecule; specifically, a metallic SWCNT with chirality 4,4 was modeled. The carvacrol, thymol, and the SWCNT were modeled using the Avogadro software [36]. Moreover, to evaluate nanotubes' functionalization, the reaction considered is depicted in Figure 1. This process was a double condensation on the SWCNT surface, adding one glucosamine in one defect, and to the other defect was added carvacrol or thymol.

The geometry of the molecules was optimized employing multiscale methods considering the partition as follows: quantum mechanics/quantum mechanics (QM/QM), specifically the ONIOM [37,38] implementation, with the higher layer at level PBE/6-31G(d,p) [34] and lower layer at the semi-empirical level (PM6) [39]. The layer was defined as follows: glucosamine, thymol, and carvacrol were selected as the higher layer (glucosamine and bioactive compounds); and the SWCNT was selected as the lower layer. Although the QM/QM method provided good tendencies in the energy evaluation, it was

to re-calculate the whole system's wave function to obtain accurate results. The above used the formalism of the density functional theory at the GGA level, with the PBE functional and the polarized triple zeta Pople [40] basis set, 6-311G(d,p), without and with empirical dispersion correction considered (Grimme D3) [41]. The binding energy ( $E_B$ ) was evaluated considering Equation (1): the energy required to form the molecule starting from the isolated atoms. The binding energy per atom was only the  $E_B/\text{number of atoms}$ .

$$E_B = E_{\text{Total}} - [\sum_{\text{atoms}} E_{\text{atoms}}]. \quad (1)$$

$$\Delta\Delta G_{\text{rx}} = \Delta G_{\text{products}} - \Delta G_{\text{reactants}}. \quad (2)$$

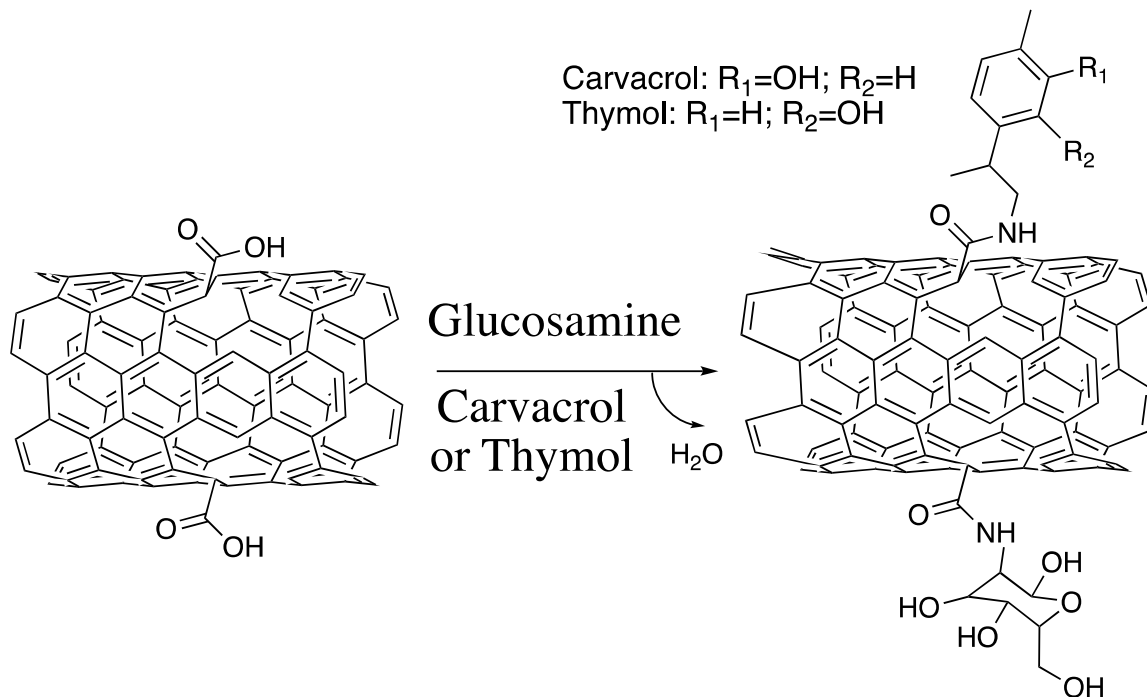


**Figure 1.** Reaction of functionalization of SWCNT44 with glucosamine and carvacrol of thymol.

Once the molecules were optimized and it was corroborated that all were at a minimum in the potential energy surface, the next step was computing the Gibbs free energy of reaction, which correlated better with the theoretical results of the experiments due to temperature and temperature entropy to the reaction energies. As well as, the whole system was evaluated using an implicit solvent, using the PCM [42] model to simulate water as a solvent in the reactions. Note that the Gibbs free energy of reaction was evaluated according to Equation (2).

Finally, in this section it is essential to mention that the global chemical descriptors were computed based on the formalism of the conceptual density functional theory [32,33,43]. The computed descriptors are: the vertical ionization potential ( $I = E_{\text{cation}} - E_{\text{neutral}}$ ), the vertical electronic affinity ( $A = E_{\text{neutral}} - E_{\text{anion}}$ ), the electronegativity ( $\chi = -(I + A)/2$ ), the hardness ( $\eta = I - A$ ), the softness ( $s = 1/\eta$ ), the electrophilicity ( $\omega = \chi^2/2\eta$ ), and the GapHOMO-LUMO energy ( $E_{\text{Gap}}$ ).

## 2.2. Solubility in Water

$$\Delta\Delta G_{\text{solv}} = \Delta G_{\text{solvent-phase}} - \Delta G_{\text{gas-phase}}. \quad (3)$$

Afterward, obtaining a stable and experimental possible system of SWCNT functionalized with the two principal bioactive molecules of oregano was proposed to perform an *in silico* assay to test the solubility in water of the studied compounds, which was

evaluated using Equation (3). At the same time, a molecular electrostatic potential analysis was carried out to evaluate the polarization of the functionalized SWCNTs.

### 2.3. Molecular Docking

Finally, an *in silico* molecular coupling was performed, considering the f-SWCNTs as the ligands and two targets. The first target was the Kallikrein *KLK5* (PDB code 2PSX) [44], which is involved in ovarian cancer, and the second target was the cyclooxygenase two (COX2, with the PDB code 3LN1 [45]), which is involved in the inflammatory process.

The molecular docking was carried out using the MolDock [46] scoring function with the Molegro Virtual Docker package (MVD) [47], considering the method employed by some of us [31,48], which has been used for SCWNT.

## 3. Results and Discussion

### 3.1. Functionalization and Binding Energies

Through the above methods, two SCWNTs were functionalized with glucosamine and with carvacrol (Carva-SWCNT-Gluc, see Figure 2A) or thymol (Thymol-SWCNT-Gluc, see Figure 2B). These were modeled and optimized, obtaining the structures depicted in Figure 2. These may not be the putative ground state on the potential energy surface, but they do not present imaginary frequencies, showing that they correspond to a stable local minimum, and considering a large number of equivalent anchor sites, probably correspond to the ground state. Note that both structures, with carvacrol and thymol, have been well modeled, avoiding the contact of the functionalizing molecules with the lateral sites of the SWCNT, which means the simulation of a larger nanotube.

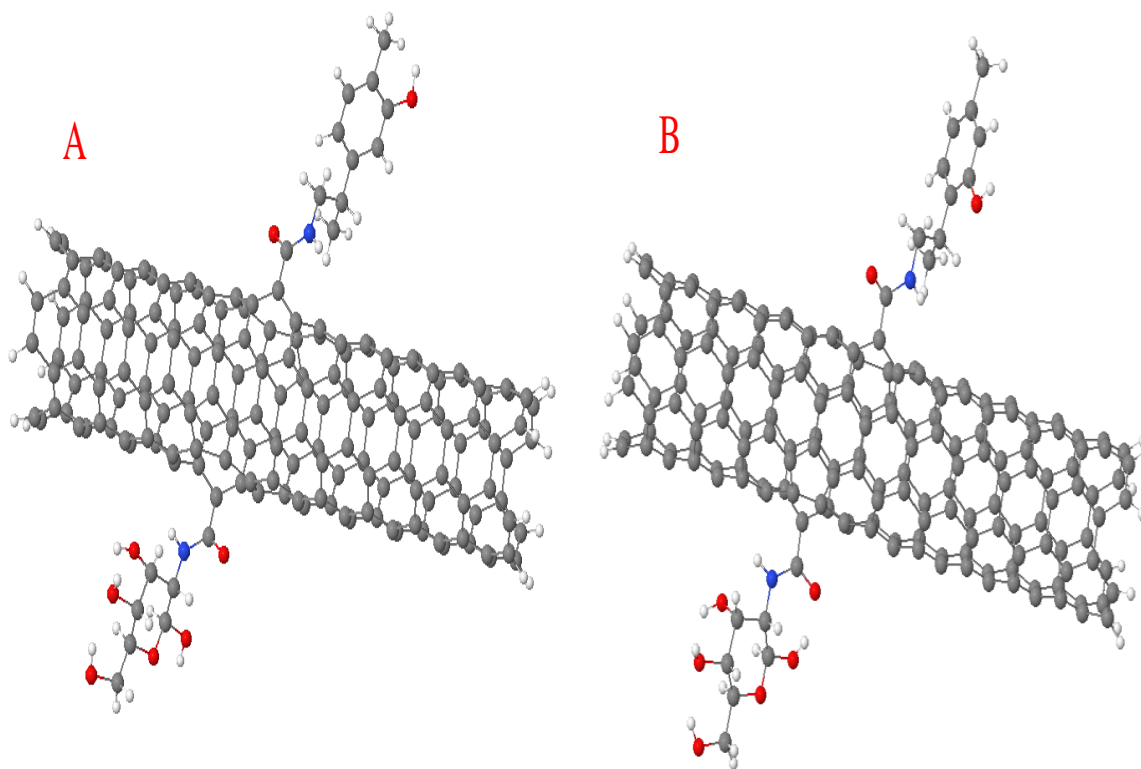


**Figure 2.** Optimized structures of (A) Carva-SWCNT-Gluc, and (B) Thymol-SWCNT-Gluc.

Regarding the SWCNT condensation, the Gibbs free energies of condensation were computed through the optimized geometries and Equation (2). Table 1 shows the above results and indicates that carvacrol and thymol reactions are exergonic and therefore present a spontaneous behavior. It is clear that the molecule with the thymol shows slightly higher exergonic behavior ( $-1.81$  eV and  $-3.06$  eV with dispersion corrections) than the

reaction carried out with the carvacrol (−1.75 eV and −2.55 with dispersion), with a 0.06 eV difference. Considering the empirical dispersion (Grimme D3 correction), the obtained values' tendency is similar. Although it is important to note that the values with Grimme corrections correspond to single-point calculations (without relaxation), a total relaxation should keep slightly different values.

**Table 1.** Gibbs free energies of functionalization of SWCNTs.

Molecule	$\Delta\Delta G_{rx}$ (eV)	
	No Dispersion	Dispersion
Carva-SWCNT-Gluc	−1.75	−2.55
Thymol-SWCNT-Gluc	−1.81	−3.06

The thymol-SWCNT-Gluc molecule has more negative values in the Gibbs free energy. Therefore, it is more likely to show a spontaneous reaction than Carva-SWCNT-Gluc; note that more negative values in the Gibbs free energies (more stable) are obtained when the dispersion correction is considered in the molecule calculations (around one eV) as seen in Table 1.

In the case of the binding energies, compared with the Gibbs free energies of functionalization, there is no difference between the Carva-SWCNT-Gluc and the Thymol-SWCNT-Gluc, presenting the same binding energies, −1996.01 eV. In the case of the binding energy per atom, the computed value is −10.40 eV/atom. Considering that carvacrol and thymol are isomers, the above can be clarified, and the binding energies, considering how long the proposed nanocarrier is, should tend to be the same.

### 3.2. Global Chemical Descriptors

Table 2 shows some global chemical descriptors computed in the present work through the conceptual DFT formalism (see the Methodology section). Electrophilicity is the global chemical descriptor encompassing all descriptors ( $\omega = \chi^2/2\eta$ ). Comparing the variation of electrophilicity in Table 2 shows an increase in this property of the f-SWCNT concerning the free bioactives. It decreases concerning the oxidized SWCNT (COOH-SWCNT44-COOH), taking values from 3.54 to 35.22 eV. The above means a stabilization in the electronic density of the SWCNT when it is functionalized, which matches with the slightly decreasing metallic behavior in non-functionalized SWCNT (with a GAP energy of 0.01). Note that the gap energy of the free drugs (values around 4 eV) is considerably decreased when coupled to the SWCNT, passing to values between 0.08 and 0.26 eV. It is worth noticing that Carva-SWCNT-Gluc has a metallic-like character while Thymol-SWCNT-Gluc has a weak insulator-like behavior.

**Table 2.** Global chemical descriptors for the studied molecules, all in eV.

Molecule	* I	A	$\chi$	$\eta$	s	$\omega$	$E_{Gap}$
Carvacrol	7.72	1.67	4.69	3.03	0.33	3.64	4.31
Thymol	7.72	1.60	4.66	3.06	0.33	3.54	4.24
Carva-SWCNT-Gluc	5.04	3.18	4.11	0.93	1.08	9.11	0.08
Thymol-SWCNT-Gluc	5.20	3.16	4.18	1.02	0.98	8.53	0.26
COOH-SWCNT44-COOH [31]	4.25	4.12	4.19	0.06	15.42	35.22	0.01

\* All the values of the table are in eV. At the same time, the vertical ionization potential (I), the vertical electronic affinity (A), the electronegativity ( $\chi$ ), the hardness ( $\eta$ ), the softness (s), the electrophilicity ( $\omega$ ), and the  $E_{GAP}$  energy ( $E_{GAP}$ ) are shown.

### 3.3. Solubility in Water

The functionalization of SWCNT has been confirmed with glucosamine and carvacrol or thymol. An exergonic behavior has been shown in both SWCNT; simultaneously, the electronic characterization was performed (as shown in Table 2). The next step is to find out the possible biocompatibility of these proposed molecules. With this aim, in the

present work the solubility of f-SWCNT in water through Equation (3) and the molecular electrostatic potential analysis were evaluated.

The Gibbs free energies of solubility in water ( $\Delta\Delta G_{\text{solv}}$ ) for f-SWCNTs are shown in Table 3. With  $\Delta\Delta G_{\text{solv}}$ , our results in water demonstrate that both proposed nanocarriers, Carva-SWCNT-Gluc and Thymol-SWCNT-Gluc, promote an increase in the free drugs' apparent solubility passing the  $\Delta\Delta G_{\text{solv}}$  of the carvacrol from  $-0.17$  eV to  $-1.28$  eV, and in the case of the thymol, this pass is from  $-0.17$  eV to  $-1.25$  eV. Note that the  $\Delta\Delta G_{\text{solv}}$  between the SWCNT structures and the free drugs are the same; this is due to the similar structures between carvacrol and thymol, which are isomers.

**Table 3.** Gibbs free energies of solubility in water.

Molecule	$\Delta\Delta G_{\text{solv}}$ (eV)
Carva-SWCNT-Gluc	$-1.28$
Thymol-SWCNT-Gluc	$-1.25$
Carvacrol	$-0.17$
Thymol	$-0.17$

Furthermore, to complete the analysis of the studied water solubility molecules', the molecular electrostatic potential surfaces (MEPS) were computed, which are depicted in Figure 3. The computed surfaces show a molecular polarization due to the relative higher electronegativity of the hydroxyl groups, which attract electronic density (depicted in the red surfaces in Figure 3). Hence, the red surfaces are very similar in both studied systems, with only a slightly higher tendency for red surfaces in the up-right site for the Carva-SWCNT-Gluc molecule, due to their hydroxyl group being located in this zone (see Figure 3A).

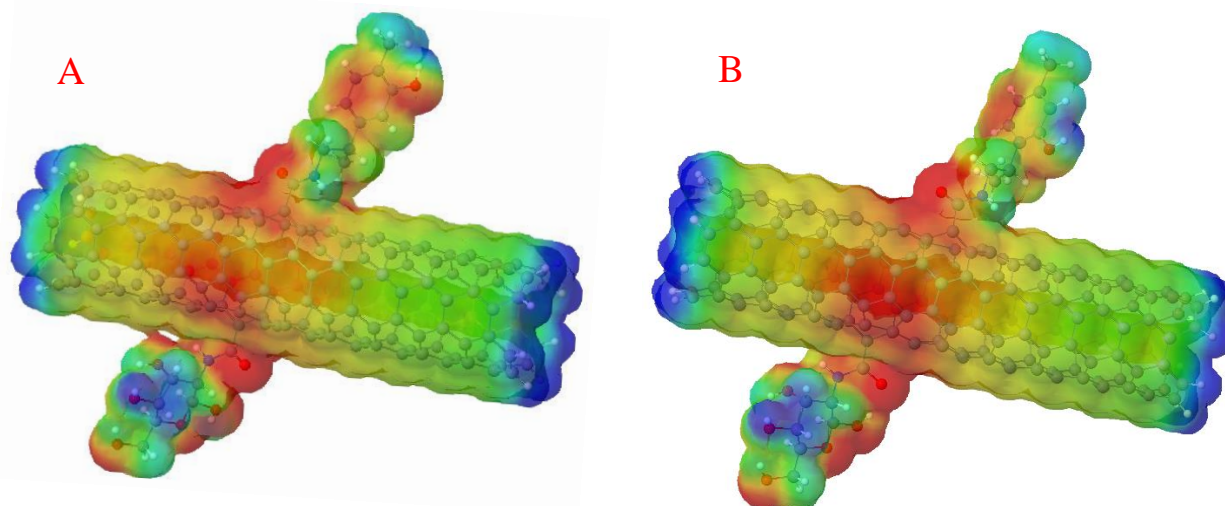


**Figure 3.** Molecular electrostatic potential surfaces for (A) Carva-SWCNT-Gluc, and (B) Thymol-SWCNT-Gluc. Red surfaces represent higher electronic density, blue surfaces indicate lower electronic density, and green surfaces depict a medium point.

Figure 3B also shows a higher polarization for the Thymol-SWCNT-Gluc molecule, with the red surface tendency to appear on the hydroxyl group, similar to the carvacrol system.

### 3.4. Molecular Docking

Finally, the present study carried the molecular docking of the Carva-SWCNT-Gluc and the Thymol-SWCNT-Gluc with two targets involved in ovarian cancer and anti-inflammatory processes: *KLK5* and *Cox2*, respectively. Figure 4 shows the preferred docking of the studied molecules into both targets, in which the ligands were optimized molecules.

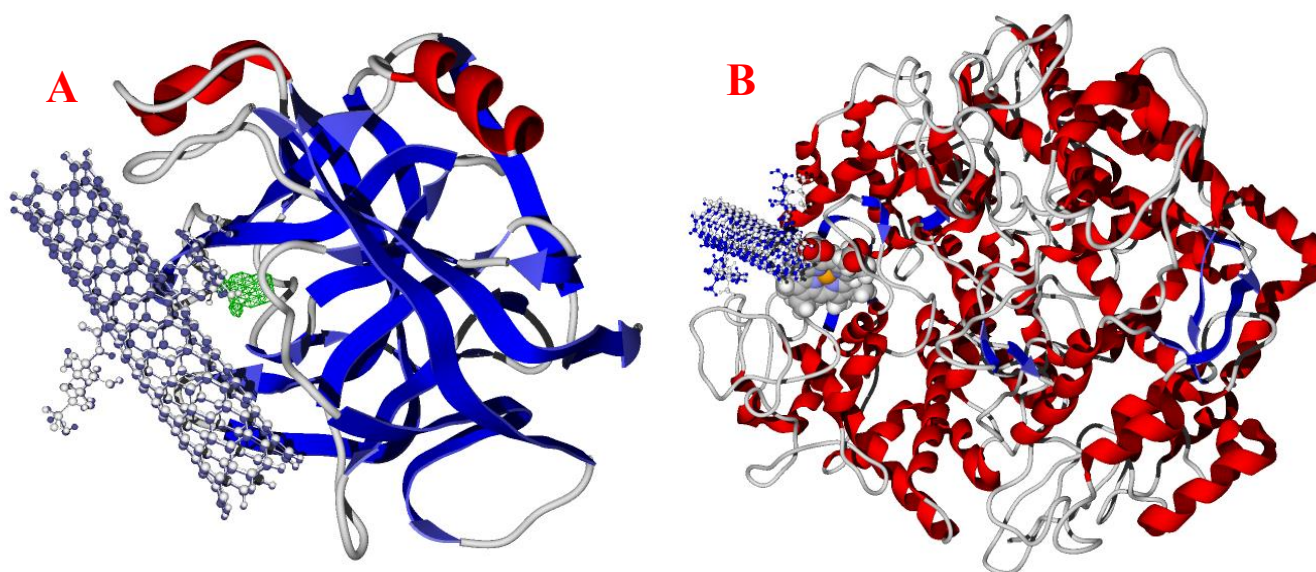


**Figure 4.** Molecular docking of Carva-SWCNT-Gluc and Thymol-SWCNT-Gluc in (A) *KLK5*, and (B) *Cox2*.

Table 4 shows the principal energies involved in the ligand-target process for the two proposed systems, Carv-SWCNT-Gluc and Thymol-SWCNT-Gluc, which can better compare with the ligand efficiency (LE). This index evaluates the energy that each atom contributes. Moreover, Thymol-SWCNT-Gluc is the preferred ligand for the *KLK5* with a LE of  $-0.08$  eV against the LE of the Carva-SWCNT-Gluc molecule ( $-0.07$  eV); the LE values are very close and it can be considered that both molecules interact similarly with this target. On the other hand, for *Cox2*, both ligands present the same LE, despite the energy values differing, and are more favorable for the Carv-SWCNT-Gluc molecule. When divided between the whole, heavy atoms are non-significant. In other words, the studied molecules can interact similarly with the selected targets.

**Table 4.** Main docking energies for the studied molecules.

Ligand	* Target	Energy	LE	Hbond	Electro	VdW
Carva-SWCNT-Gluc	<i>KLK5</i>	$-14.92$	$-0.07$	$-0.05$	$0.01$	$23.06$
	<i>Cox2</i>	$-22.63$	$-0.11$	$-0.26$	$-0.05$	$-0.59$
Thymol-SWCNT-Gluc	<i>KLK5</i>	$-16.70$	$-0.08$	$-0.05$	$-0.05$	$8.39$
	<i>Cox2</i>	$-22.08$	$-0.11$	$-0.11$	$-0.08$	$-1.31$

\* All the values of the table are in eV. LE is the ligand efficiency ( $LE = \text{Energy}/\text{No. of heavy atoms}$ ), Hbond means the hydrogen bond energy, Electro represents the electrostatic interactions, and VdW is the Van der Waals interactions.

Finally, to understand better the interactions of the proposed molecules, Figure 5A depicts the hydrogen bond interactions between Carva-SWCNT-Gluc and *KLK5*, which is through Ser195 and His57 with the hydroxyl of carvacrol, and with the glucosamine with Tyr219. Figure 5B shows the higher electrostatic attraction between the SWCNT of Thymol-SWCNT-Gluc with the co-factor of *Cox2* (HEM group), and the repulsion and attraction between Lys391, the thymol hydroxyl group.

Therefore, the above results show a possible carvacrol and thymol carrier using a metallic single wall carbon nanotube, an advantage of the SWCNT interaction with the co-factor of *Cox2*, and the possibility of delivering the oregano bioactives to cancer and anti-inflammatory targets.

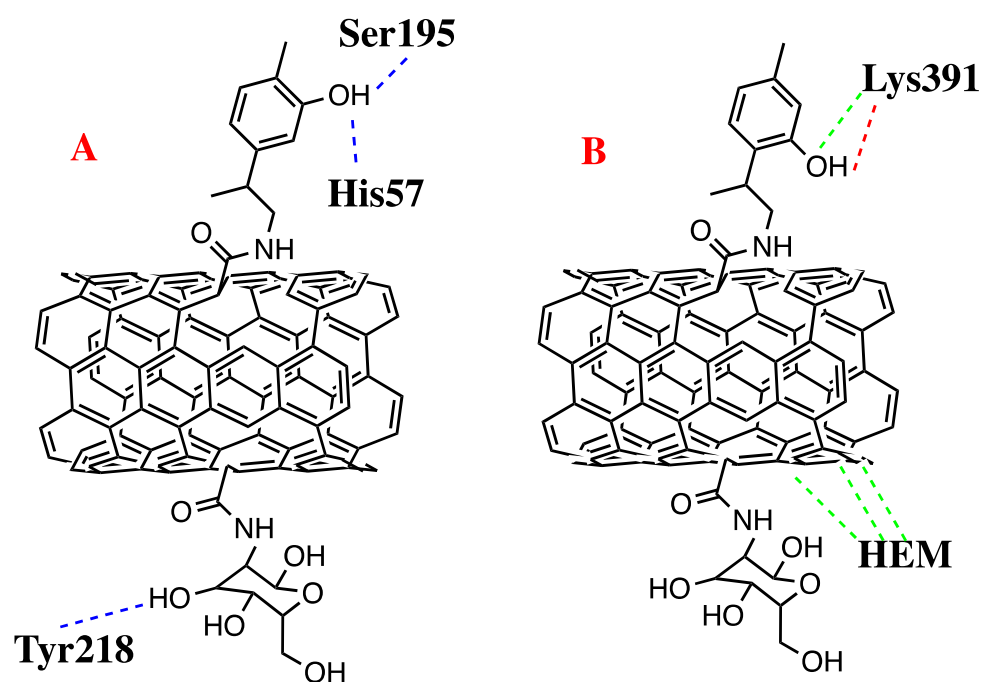


**Figure 5.** (A) Hydrogen bond interactions of Carva-SWCNT-Gluc with *KLK5*, and (B) electrostatic interactions of Thymol-SWCNT-Gluc with *Cox2*. Blue lines represent the Hbond interactions, green lines the attractive electrostatic interactions, and red lines depict the repulsive electrostatic interactions.

#### 4. Conclusions

The two main bioactive molecules of oregano (carvacrol and thymol) were modeled and optimized using multiscale and DFT methods; these were linked to a finite size model of a metallic single wall carbon nanotube, and added a molecule that promotes the solubility in water of the system (glucosamine). The results show that the proposed molecules, Carva-SWCNT-Gluc and Thymol-SWCNT-Gluc, can be synthesized with the exposed condensation reaction, with an exergonic and spontaneous behavior,  $-1.75$  eV and  $-1.81$  eV, respectively. The studied molecules were subjected to an electronic characterization, considering the global descriptors based on the conceptual DFT formalism. The above demonstrates the increase in gap energy means a decrease in electrophilicity for the f-SWCNT concerning the oxidized SWCNT. In addition, there is a decrease in the gap and increase in electrophilicity compared with the free drugs, promoting an electronic stabilization in the f-SWCNT formation. Furthermore, the results show that the studied molecules can present a possible biocompatibility due to the higher polarization of the molecule and the increase in apparent solubility. Finally, the interaction of Carva-SWCNT-Gluc and Thymol-SWCNT-Gluc against cancer and anti-inflammatory targets shows that these interactions are favorable due to their hydrogen bond and electrostatic interactions.

The proposed f-SWCNT is one of the possible nanocarriers of carvacrol and thymol capable of delivering the oregano bioactives to selected targets, and promoting the putative apoptosis of neoplastic cells while regulating the inflammation process.

**Author Contributions:** Conceptualization and methodology, E.D.-C.; validation, formal analysis, investigation, F.A.-G.; resources, writing—original draft preparation, A.M.-R.; writing—review and editing, E.D.-C.; visualization, supervision, F.A.-G. All authors have read and agreed to the published version of the manuscript.

**Funding:** This research received no external funding.

**Data Availability Statement:** Not applicable.

**Acknowledgments:** We acknowledge to the Laboratorio Nacional de Caracterización de Propiedades Físicoquímicas y Estructura Molecular (UG-UAA-CONACYT, Project: 123732) for the computing time provided at the PIPILA cluster.

**Conflicts of Interest:** The authors declare no conflict of interest.

## References

1. Gautam, N.; Mantha, A.K.; Mittal, S. Essential oils and their constituents as anticancer agents: A mechanistic view. *BioMed Res. Int.* **2014**, *1*, 154106. [[CrossRef](#)] [[PubMed](#)]
2. Dai, W.; Sun, C.; Huang, S.; Zhou, Q. Carvacrol suppresses proliferation and invasion in human oral squamous cell carcinoma. *Oncotargets Ther.* **2016**, *9*, 2297–2304. [[CrossRef](#)] [[PubMed](#)]
3. Portillo-Ruiz, M.C.; Sánchez, R.A.S.; Ramos, S.V.; Muñoz, J.V.T.; Nevárez-Moorillón, G.V. Antifungal effect of Mexican oregano (*Lippia berlandieri* Schauer) essential oil on a wheat flour-based Medium. *J. Food Sci.* **2012**, *77*, M441–M445. [[CrossRef](#)] [[PubMed](#)]
4. Elshafie, H.S.; Camele, I. An overview of the biological effects of some mediterranean essential oils on human health. *BioMed Res. Int.* **2017**, *1*, 9268468. [[CrossRef](#)]
5. Lambert, R.J.W.; Skandamis, P.N.; Coote, P.J.; Nychas, G.J. A study of the minimum inhibitory concentration and mode of action of oregano essential oil, thymol and carvacrol. *J. Appl. Microbiol.* **2001**, *91*, 453–462. [[CrossRef](#)]
6. Zengin, H.; Baysal, A.H. Antibacterial and antioxidant activity of essential oil terpenes against pathogenic and spoilage-forming bacteria and cell structure-activity relationships evaluated by SEM microscopy. *Molecules* **2014**, *19*, 17773–17798. [[CrossRef](#)]
7. Sarac, N.; Ugur, A. Antimicrobial activities of the essential oils of *Origanum onites* L., *Origanum vulgare* L. subspecies *hirtum* (Link) Ietswaart, *Satureja thymbra* L., and *Thymus cilicicus* Boiss. & Bal. growing wild in Turkey. *J. Med. Food* **2008**, *11*, 568–573.
8. Prieto, J.M.; Lacopini, P.; Cioni, P.; Chericoni, S. In vitro activity of the essential oils of *Origanum vulgare*, *Satureja montana* and their main constituents in peroxynitrite-induced oxidative processes. *Food Chem.* **2007**, *104*, 889–895. [[CrossRef](#)]
9. Fachini-Queiroz, F.C.; Kummer, R.; Estevao-Silva, C.F.; Carvalho, M.D.D.B.; Cunha, J.M.; Grespan, R.; Cuman, R.K.N. Effects of thymol and carvacrol, constituents of *Thymus vulgaris* L. essential oil, on the inflammatory response. *Evid.-Based Compl. Alt.* **2012**, *1*, 657026.
10. Sobral, M.V.; Xavier, A.L.; Lima, T.C.; De Sousa, D.P. Antitumor activity of monoterpenes found in essential oils. *Sci. World J.* **2014**, *1*, 953451. [[CrossRef](#)]
11. Elbe, H.; Yigitturk, G.; Cavusoglu, T.; Baygar, T.; Ozgul Onal, M.; Ozturk, F. Comparison of ultrastructural changes and the anticarcinogenic effects of thymol and carvacrol on ovarian cancer cells: Which is more effective? *Ultrastruct. Pathol.* **2020**, *44*, 193–202. [[CrossRef](#)] [[PubMed](#)]
12. Burt, S. Essential oils: Their antibacterial properties and potential applications in foods—a review. *Int. J. Food Microbiol.* **2004**, *94*, 223–253. [[CrossRef](#)] [[PubMed](#)]
13. Trombetta, D.; Castelli, F.; Sarpietro, M.G.; Venuti, V.; Cristani, M.; Daniele, C.; Saija, A.; Mazzanti, G.; Bisignano, G. Mechanisms of antibacterial action of three monoterpenes. *Antimicrob. Agents Chemother.* **2005**, *49*, 2474–2478. [[CrossRef](#)]
14. Ortega-Nieblas, M.M.; Robles-Burgueño, M.R.; Acedo-Félix, E.; González-León, A.; Morales-Trejo, A.; Vázquez-Moreno, L. Chemical composition and antimicrobial activity of oregano (*Lippia palmeri* S. Wats) essential oil. *Rev. Fitotec. Mex.* **2011**, *34*, 11–17. [[CrossRef](#)]
15. Nostro, A.; Papalia, T. Antimicrobial activity of carvacrol: Current progress and future perspectives. *Recent Pat. Antiinfect. Drug Discov.* **2012**, *7*, 28–35. [[CrossRef](#)] [[PubMed](#)]
16. Nagoor-Meeran, M.F.; Javed, H.; Al-Tae, H.; Azimullah, S.; Ojha, S.K. Pharmacological properties and molecular mechanisms of thymol: Prospects for its therapeutic potential and pharmaceutical development. *Front. Pharmacol.* **2017**, *8*, 380. [[CrossRef](#)]
17. Can-Baser, K.H. Biological and pharmacological activities of carvacrol and carvacrol bearing essential oils. *Curr. Pharm. Des.* **2008**, *14*, 3106–3119. [[CrossRef](#)] [[PubMed](#)]
18. Ben-Arfa, A.; Combes, S.; Preziosi-Belloy, L.; Gontard, N.; Chalier, P. Antimicrobial activity of carvacrol related to its chemical structure. *Lett. Appl. Microbiol.* **2006**, *43*, 149–154. [[CrossRef](#)]
19. Ultee, A.; Kets, E.P.; Alberda, M.; Hoekstra, F.A.; Smid, E.J. Adaptation of the food-borne pathogen *Bacillus cereus* to carvacrol. *Arch. Microbiol.* **2000**, *174*, 233–238. [[CrossRef](#)]
20. Di Pasqua, R.; Hoskins, N.; Betts, G.; Mauriello, G. Changes in membrane fatty acids composition of microbial cells induced by addition of thymol, carvacrol, limonene, cinnamaldehyde, and eugenol in the growing media. *J. Agric. Food Chem.* **2006**, *54*, 2745–2749. [[CrossRef](#)]
21. Cristani, M.; D’Arrigo, M.; Mandalari, G.; Castelli, F.; Sarpietro, M.G.; Micieli, D.; Trombetta, D. Interaction of four monoterpenes contained in essential oils with model membranes: Implications for their antibacterial activity. *J. Agric. Food Chem.* **2007**, *55*, 6300–6308. [[CrossRef](#)] [[PubMed](#)]
22. Arunasree, K.M. Anti-proliferative effects of carvacrol on a human metastatic breast cancer cell line, MDA-MB 231. *Phytomedicine* **2010**, *17*, 581–588. [[CrossRef](#)] [[PubMed](#)]
23. Fan, K.; Li, X.; Cao, Y.; Qi, H.; Li, L.; Zhang, Q.; Sun, H. Carvacrol inhibits proliferation and induces apoptosis in human colon cancer cells. *Anticancer. Drugs* **2015**, *26*, 813–823. [[CrossRef](#)] [[PubMed](#)]

24. Khan, I.; Bahuguna, A.; Kumar, P.; Bajpai, V.K.; Kang, S.C. In vitro and in vivo antitumor potential of carvacrol nanoemulsion against human lung adenocarcinoma A549 cells via mitochondrial mediated apoptosis. *Sci. Rep.* **2018**, *8*, 144. [[CrossRef](#)] [[PubMed](#)]
25. Aguilar-Pérez, K.M.; Medina, D.I.; Narayanan, J.; Parra-Saldívar, R.; Iqbal, H.M.N. Synthesis and Nano-Sized Characterization of Bioactive Oregano Essential Oil Molecule-Loaded Small Unilamellar Nanoliposomes with Antifungal Potentialities. *Molecules* **2021**, *26*, 2880. [[CrossRef](#)] [[PubMed](#)]
26. Kang, S.H.; Kim, Y.S.; Kim, E.K.; Hwang, J.W.; Jeong, J.H.; Dong, X.; Park, P.J. Anticancer effect of thymol on AGS human gastric carcinoma cells. *J. Microbiol. Biotechnol.* **2016**, *26*, 28–37. [[CrossRef](#)] [[PubMed](#)]
27. Kalembe, D.A.A.K.; Kunicka, A. Antibacterial and antifungal properties of essential oils. *Current medicinal chemistry. Curr. Med. Chem.* **2003**, *10*, 813–829. [[CrossRef](#)]
28. Liolios, C.C.; Gortzi, O.; Lalas, S.; Tsaknis, J.; Chinou, I. Liposomal incorporation of carvacrol and thymol isolated from the essential oil of *Origanum dictamnus* L. and in vitro antimicrobial activity. *Food Chem.* **2009**, *112*, 77–83. [[CrossRef](#)]
29. Coimbra, M.; Isacchi, B.; van Bloois, L.; Torano, J.S.; Ket, A.; Wu, X.; Bilia, R. Improving solubility and chemical stability of natural compounds for medicinal use by incorporation into liposomes. *Int. J. Pharm.* **2011**, *416*, 433–442. [[CrossRef](#)]
30. Diaz-Cervantes, E.; García-Revilla, M.A.; Robles, J.; Aguilera-Granja, F. Solubility of functionalized single-wall carbon nanotubes in water: A theoretical study. *Theor. Chem. Acc.* **2017**, *136*, 127. [[CrossRef](#)]
31. Diaz-Cervantes, E.; Robles, J.; Aguilera-Granja, F. Understanding the structure, electronic properties, solubility in water, and protein interactions of three novel nano-devices against ovarian cancer: A computational study. *J. Nanopart. Res.* **2018**, *20*, 266. [[CrossRef](#)]
32. Parr, R.G.; Yang, W. *Density Functional Theory of Atoms and Molecules*, 1st ed.; Oxford Science Publications: Cary, NC, USA, 1989.
33. Parr, R.G.; Pearson, R.G. Absolute hardness: Companion parameter to absolute electronegativity. *J. Am. Chem. Soc.* **1983**, *105*, 7512–7516. [[CrossRef](#)]
34. Perdew, J.P.; Burke, K.; Ernzerhof, M. Generalized Gradient Approximation Made Simple. *Phys. Rev. Lett.* **1996**, *77*, 3865–3868. [[CrossRef](#)]
35. Frisch, M.J.; Pople, J.A.; Binkley, J.S. Self-consistent molecular orbital methods 25. Supplementary functions for Gaussian basis sets. *J. Chem. Phys.* **1984**, *80*, 3265–3269. [[CrossRef](#)]
36. *Avogadro: An Open-Source Molecular Builder and Visualization Tool*, Version 1.2.0.
37. Svensson, M.; Humbel, S.; Froese, R.D.J.; Matsubara, T.; Sieber, S.; Morokuma, K. ONIOM: A Multilayered Integrated MO + MM Method for Geometry Optimizations and Single Point Energy Predictions. A Test for Diels–Alder Reactions and Pt(P(t-Bu)<sub>3</sub>)<sub>2</sub> + H<sub>2</sub> Oxidative Addition. *J. Phys. Chem* **1996**, *100*, 19357–19363. [[CrossRef](#)]
38. Humbel, S.; Sieber, S.; Morokuma, K. The IMOMO method: Integration of different levels of molecular orbital approximations for geometry optimization of large systems: Test for n-butane conformation and S<sub>N</sub>2 reaction: RCl + Cl<sup>-</sup>. *J. Chem. Phys.* **1996**, *105*, 1959–1967. [[CrossRef](#)]
39. Stewart, J.J.P. Optimization of parameters for semiempirical methods V: Modification of NDDO approximations and application to 70 elements. *J. Mol. Mod.* **2007**, *13*, 1173–1213. [[CrossRef](#)] [[PubMed](#)]
40. Binkley, J.S.; Pople, J.A.; Hehre, W.J. Self-Consistent Molecular Orbital Methods. 21. Small Split-Valence Basis Sets for First-Row Elements. *J. Am. Chem. Soc.* **1980**, *102*, 939–947. [[CrossRef](#)]
41. Schwabe, T.; Grimme, S. Theoretical thermodynamics for large molecules: Walking the thin line between accuracy and computational cost. *Acc. Chem. Res.* **2008**, *41*, 569–579. [[CrossRef](#)]
42. Onsager, L. Electric Moments of Molecules in Liquids. *J. Am. Chem. Soc.* **1936**, *58*, 1486–1493. [[CrossRef](#)]
43. Lee, C.; Yang, W.; Parr, R.G. Development of the Colle-Salvetti correlation-energy formula into a functional of the electron density. *Phys. Rev. B* **1988**, *37*, 785–789. [[CrossRef](#)] [[PubMed](#)]
44. Yousef, G.M.; Obiezu, C.V.; Jung, K.; Stephan, C.; Scorilas, A.; Diamandis, E.P. Differential expression of kallikrein gene 5 in cancerous and normal testicular tissues. *Urology* **2002**, *60*, 714–718. [[CrossRef](#)]
45. Wang, J.L.; Limburg, D.; Matthew, J.; Graneto, J.; Springer, J.; Hamper, J.R.B.; Liao, S.; Pawlitz, J.L.; Kurumbail, R.G.; Maziasz, T.; et al. The novel benzopyran class of selective cyclooxygenase-2 inhibitors. Part 2: The second clinical candidate having a shorter and favorable human half-life. *Bioorg. Med. Chem. Lett.* **2010**, *20*, 7159–7163. [[CrossRef](#)]
46. Thomsen, R.; Christensen, M.H. MolDock: A new technique for high-accuracy molecular docking. *J. Med. Chem.* **2006**, *49*, 3315–3321. [[CrossRef](#)] [[PubMed](#)]
47. Yang, J.; Chen, C. GEMDOCK: A generic evolutionary method for molecular docking. *Proteins* **2004**, *55*, 288–304. [[CrossRef](#)] [[PubMed](#)]
48. Villaseñor-Granados, T.; Díaz-Cervantes, E.; Soto-Arredondo, K.J.; Martínez-Alfaro, M.; Robles, J.; García-Revilla, M.A. Binding of Pb-Melatonin and Pb-(Melatonin-metabolites) complexes with DMT1 and ZIP8: Implications for lead detoxification. *DARU* **2019**, *27*, 137–148. [[CrossRef](#)] [[PubMed](#)]